

Atomic data from the IRON Project

XXI. Electron excitation of fine-structure transitions involving the $3d^6 4s^2 \ ^5D$ ground state and the $3d^7 4s \ ^5F$ metastable state of Fe I

J. Pelan and K.A. Berrington

Department of Applied Mathematics & Theoretical Physics, The Queen's University, Belfast, BT7 1NN, UK

Received June 19; accepted July 15, 1996

Abstract. Low energy electron excitation collision strengths for fine-structure transitions involving the $3d^6 4s^2 \ ^5D_J$ ground term and the $3d^7 4s \ ^5F_J$ first excited term of neutral Fe are calculated. The model target atom includes the lowest three terms ($\ ^5D$, $\ ^5F$ and $\ ^3F$) together with four pseudostates ($\ ^5P^\circ$, $\ ^5D^\circ$, $\ ^5F^\circ$, $\ ^5G^\circ$) chosen to represent the dipole polarizability of the ground term and first excited term of Fe. The Breit-Pauli R-matrix method is used to calculate the fine-structure collision strength, which is averaged over a Maxwellian velocity distribution to obtain effective collision strengths as a function of electron temperature in the range 100 – 4000 K. The low-temperature form of the collision strength is established for the first time for Fe I.

Key words: atomic data

1. Introduction

The aim of this paper is to calculate low-temperature electron excitation data for atomic iron (Fe I). This involves establishing the near-threshold behaviour of the collision strength, a challenging problem in theoretical atomic physics.

Fe I is a particularly interesting and testing case. It is present in many types of cool or cold plasma, e.g. laboratory-produced plasmas, K-type and M-type stars, the interstellar media, and supernovae remnants such as SN 1987A where Fe I infrared emission lines have been observed (Li et al. 1993). The difficulties for the atomic theoretician are that many effects have to be taken into account at low energies, e.g. fine-structure, long-range polarization, and channel coupling between nearby states. A further difficulty is associated with computing the algebra for such a complex open d-shell atomic system.

Send offprint requests to: J. Pelan

Consider the first three terms in Fe I ($3d^6 4s^2 \ ^5D$, $3d^7 4s \ ^5F$, $3d^7 4s \ ^3F$), whose energies span the range up to 0.12 Ryd. above the $\ ^5D$ ground state. This is clearly the minimum number of terms that need to be included in a close-coupling formulation, in order to obtain effective collision strengths over a reasonable temperature range (say up to 4000 K, ≈ 0.025 Ryd).

However, data are also required for applications at much lower temperatures (below 1000 K), comparable to the fine-structure splittings. At very low electron energies, large radial distances play an important role, and long-range polarization effects are important (Berrington 1988). Also the spin-orbit interaction is strong in the collisional Hamiltonian, and a proper treatment must account for the kinematics of the scattering electron in the different fine-structure channels.

This work is part of an international collaboration known as the IRON Project (Hummer et al. 1993, referred to as Paper I) to obtain accurate collision rates for fine-structure transitions. A full list of these papers published to-date is included in the references.

2. The calculation

Collision strengths are calculated using the Breit-Pauli version of the R-matrix method (Scott & Taylor 1982), following a similar procedure to that of Berrington (1988), who studied atomic oxygen.

The target wavefunctions are constructed from 1s, 2s, 2p, 3s, 3p, 3d, 4s, $\bar{4}p$ and $\bar{4}d$ orbitals; The 1s through 4s radial orbitals are from Clementi & Roetti (1974), optimised on the $3d^6 4s^2 \ ^5D$ ground state. The $\bar{4}d$ correlation orbital is optimised on the $3d^7 4s \ ^5,^3F$ states using Hibbert's (1975) program CIV3, in order to account for the different radial distribution of the d-orbital in the ground and excited states. This improved the term energy splitting of the states.

Long-range polarization effects are included by introducing the pseudostates ($\ ^5P^\circ$, $\ ^5D^\circ$, $\ ^5F^\circ$, $\ ^5G^\circ$), each of

which involves a $\bar{4}p$ pseudo-orbital. The first three pseudostates are chosen to represent the dipole polarizability of the 5D ground state; that is, the $\bar{4}p$ orbital and the pseudostate eigenvectors are optimised on the polarizability using program CIVPOL (Hibbert et al. 1977). The fourth pseudostate, ${}^5G^\circ$, is inserted to include as much as possible of the dipole polarizability of the 5F metastable state. With these pseudostates, the calculated dipole polarizability of the 5D ground state is 92.58 au, and of the 5F state is 61.42 au.

To estimate the true polarizability, two previous R-matrix photoionization calculations were used, namely the Fe^+ targets of Sawey & Berrington (1992) and of Bautista (1996). The static dipole polarizability (calculated using the R-matrix programs: Berrington et al. 1996) of the 5D ground state was found to be 104.36 and 103.83 au respectively which shows excellent agreement between both calculations. This means that 89% of the ground state polarizability is accounted for in the Fe I target.

The $\bar{4}p$ and $\bar{4}d$ orbitals generated and used for this calculation are tabulated in Table 1. The configurations used in each target state are in Table 2. There are of course many more configurations allowable in LS coupling for each symmetry, but only those making a significant contribution are retained.

These four pseudostates, together with the three physical states (5D , 5F , 3F) give rise to 31 fine-structure levels, which are explicitly included in the R-matrix calculation (see Table 3). Configuration-interaction wavefunctions are used for the target states; considerable effort is needed to handle the resulting open d-shell atomic system in the collision calculation. In particular, $(N+1)$ -electron configurations are restricted to certain d-shell couplings, such as $3d^6({}^5D)4l4'l''$.

The collision strengths were calculated using the FARM packaged developed by Burke & Noble (1995).

Table 1. $\bar{4}p$ and $\bar{4}d$ radial orbitals used in the Fe R-matrix calculation (the remaining target orbitals are from Clementi & Roetti 1975). Each orbital is in the form $P(r) = \sum_i c_i r^{n_i} \exp(-\zeta_i r)$

$P(r)$	c_i	n_i	ζ_i
$\bar{4}p$	1.94677	2	0.784
	-9.92782	3	2.666
	-1.18898	4	1.469
$\bar{4}d$	43.52606	3	4.92518
	-0.31262	4	1.26745

Table 2. Configurations used in the Fe I target term expansions. (All ${}^{2S+1}L$ combinations are assumed unless otherwise stated)

Term	Configurations			
5D	$3d^6 4s^2$	$3d^6({}^5D)4s\bar{4}d$		
5F	$3d^7 4s$	$3d^6({}^5D)4s\bar{4}d$	$3d^6 4s({}^4L)\bar{4}d$	
3F	$3d^7 4s$	$3d^6({}^5D)4s\bar{4}d$	$3d^6 4s({}^2L)\bar{4}d$	$3d^6 4s^2$
$\bar{5}P^\circ$	$3d^6({}^5D)4s\bar{4}p$	$3d^5({}^6S)4s^2\bar{4}p$	$3d^6({}^5D)\bar{4}p\bar{4}d$	
$\bar{5}D^\circ$	$3d^6({}^5D)4s\bar{4}p$	$3d^7({}^4F)\bar{4}p$	$3d^6({}^5D)\bar{4}p\bar{4}d$	
$\bar{5}F^\circ$	$3d^6({}^5D)4s\bar{4}p$	$3d^7({}^4F)\bar{4}p$	$3d^6({}^5D)\bar{4}p\bar{4}d$	
$\bar{5}G^\circ$	$3d^7({}^4F)\bar{4}p$	$3d^6({}^5D)4s\bar{4}p$		

Table 3. Fine-structure energy levels of the states of Fe I included in the R-matrix calculation, in Rydberg units. Observed energies are from Reader & Sugar (1975)

Term	J	Present	Observed	Index
$3d^6 4s^2 {}^5D$	4	0.0	0.0	1
	3	0.0044	0.0046	2
	2	0.0076	0.0077	3
	1	0.0097	0.0097	4
	0	0.0108	0.0107	5
$3d^7 4s {}^5F$	5	0.0564	0.0760	6
	4	0.0608	0.0810	7
	3	0.0642	0.0848	8
	2	0.0667	0.0876	9
	1	0.0685	0.0895	10
$3d^7 4s {}^3F$	4	0.1209	0.1314	11
	3	0.1263	0.1378	12
	2	0.1304	0.1423	13
$\bar{5}D^\circ$		0.3277		
$\bar{5}F^\circ$		0.3376		
$\bar{5}P^\circ$		0.3386		
$\bar{5}G^\circ$		0.3477		

3. Results

The calculated collision strengths (Ω) for fine-structure transitions involving the 5D ground state and the 5F metastable state are averaged over a Maxwellian velocity distribution to obtain effective collision strengths (Υ) as a function of electron temperature in the range 100 – 4000 K. This procedure is detailed in Paper I. The results are shown in Tables 4 and 5.

An example plot of one particular collision strength $\Omega({}^5D_4, {}^5D_3)$ is shown in Fig. 1. Some resonance features can be seen due to excitation into states of Fe^- .

The figure also demonstrates that the collision strength exhibits Wigner threshold behaviour (Wigner 1948) of the form $\Omega(i, j) \sim E^{l+1/2}$ where l is the dominant angular momentum contribution, i.e. $l = 0$ for s-wave, $l = 1$ for

Table 4. Effective collision strengths $\Upsilon(i, j)$ for electron excitation up to the first 10 J levels of Fe I, initial levels 1,2 & 3. We use the notation $x \pm n$ to indicate the number $x \times 10^{\pm n}$

Transition	Temperature (Log K)				
	2.0	2.4	2.8	3.2	3.6
1-2	2.01-2	3.38-2	7.05-2	2.44-1	7.65-1
1-3	4.27-2	9.47-2	1.55-1	2.28-1	3.44-1
1-4	1.06-4	4.30-4	1.74-3	1.31-2	3.35-2
1-5	2.39-7	1.14-6	3.72-5	1.02-3	2.72-3
1-6	2.62-2	7.72-2	1.83-1	4.30-1	8.24-1
1-7	1.84-2	4.32-2	9.15-2	1.92-1	3.32-1
1-8	8.61-3	1.84-2	3.79-2	7.78-2	1.26-1
1-9	2.56-3	5.96-3	1.25-2	2.38-2	3.44-2
1-10	6.73-5	2.00-4	4.86-4	1.02-3	1.50-3
2-3	1.76-2	4.75-2	1.07-1	2.73-1	7.20-1
2-4	1.09-2	2.16-2	3.41-2	8.07-2	2.35-1
2-5	3.97-5	1.71-4	8.71-4	1.06-2	3.38-2
2-6	9.05-3	2.56-2	5.69-2	1.31-1	2.64-1
2-7	1.51-2	3.49-2	7.38-2	1.64-1	3.04-1
2-8	1.72-2	3.76-2	7.98-2	1.67-1	2.78-1
2-9	9.57-3	2.19-2	4.63-2	9.65-2	1.57-1
2-10	2.31-3	6.13-3	1.28-2	2.46-2	3.68-2
3-4	7.72-3	2.25-2	5.39-2	1.46-1	4.02-1
3-5	2.11-4	9.84-4	4.39-3	3.24-2	1.45-1
3-6	2.56-3	6.77-3	1.31-2	2.54-2	4.82-2
3-7	7.91-3	1.88-2	4.17-2	1.00-1	2.03-1
3-8	1.50-2	2.96-2	5.51-2	1.08-1	1.83-1
3-9	1.51-2	3.60-2	7.62-2	1.45-1	2.18-1
3-10	6.07-3	1.65-2	3.59-2	7.63-2	1.27-1

Table 5. Effective collision strengths $\Upsilon(i, j)$ for electron excitation up to the first 10 J levels of Fe I, initial levels 4 to 9. We use the notation $x \pm n$ to indicate the number $x \times 10^{\pm n}$

Transition	Temperature (Log K)				
	2.0	2.4	2.8	3.2	3.6
4-5	1.86-4	5.94-4	2.42-3	2.06-2	9.76-2
4-6	8.99-7	2.91-6	8.26-6	2.46-5	5.72-5
4-7	5.55-3	1.16-2	2.04-2	3.72-2	6.55-2
4-8	4.43-3	1.01-2	2.37-2	5.78-2	1.13-1
4-9	1.21-2	2.44-2	4.36-2	8.00-2	1.29-1
4-10	9.67-3	2.74-2	5.82-2	1.05-1	1.52-1
5-6	3.66-9	3.48-8	2.97-7	1.40-6	4.13-6
5-7	2.85-8	1.64-7	1.21-6	7.80-6	2.66-5
5-8	4.49-3	8.31-3	1.40-2	2.56-2	4.46-2
5-9	1.93-3	5.20-3	1.29-2	3.07-2	5.70-2
5-10	1.89-3	4.77-3	9.32-3	1.84-2	3.10-2
6-7	2.47-2	5.41-2	1.02-1	2.00-1	3.75-1
6-8	8.89-4	2.18-3	5.53-3	1.46-2	2.91-2
6-9	1.10-5	4.39-5	1.86-4	7.27-4	1.77-3
6-10	1.30-8	1.41-7	2.24-6	2.71-5	1.02-4
7-8	5.53-2	1.08-1	1.87-1	3.27-1	5.33-1
7-9	8.57-4	2.25-3	5.79-3	1.56-2	3.16-2
7-10	6.36-6	2.81-5	1.23-4	5.27-4	1.38-3
8-9	5.73-2	1.19-1	2.12-1	3.70-1	5.89-1
8-10	4.44-4	1.44-3	3.97-3	1.12-2	2.31-2
9-10	2.93-2	7.64-2	1.49-1	2.78-1	4.49-1

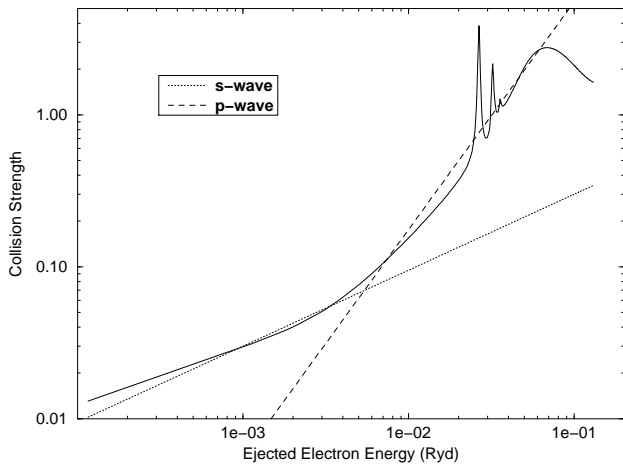


Fig. 1. Log – log plot of collision strength $\Omega(^5D_4, ^5D_3)$, solid line, with fits showing the forms of the Wigner threshold behaviour, dotted & dashed lines

p-wave etc. At the lowest energies the s-wave dominates but as the energy approaches the next thresholds the p-wave contribution becomes evident. The approximate fits are $\Omega = 0.95 E^{1/2}$ for the s-wave (0.0 to 0.004 Ryd) and $\Omega = 176 E^{3/2}$ for the p-wave (0.004 to 0.07 Ryd). All 45 transitions exhibit similar behaviour although clearly for different values of l and energy.

4. Conclusions

The effective collision strengths for the fine-structure transitions between the ground and first excited states of neutral iron have been calculated for the first time. Due to the truncation of the close-coupling basis and incomplete dipole polarizability of the target, errors are estimated to be in the region of 10 to 20%

Acknowledgements. This work was done with the support of a PPARC grant GR/H93576, and an EC network contract ERB CHRX CT920013. The authors would like to thank Dr. Bautista for providing data files for the polarization calculation.

References

(IRON Project papers are indicated in brackets)
 Bautista M.A., 1996, A&AS (Paper XX) (in press)
 Bautista M.A., Pradhan A.K., 1996, A&AS 115, 551 (Paper XIII)

- Berrington K.A., 1988, *J. Phys. B: At. Mol. Opt. Phys.* 21, 1083
- Berrington K.A., 1995, *A&AS* 109, 193 (Paper VIII)
- Berrington K.A., Pelan J.C., 1995, *A&AS* 114, 367 (Paper XII)
- Berrington K.A., Eissner W.B., Norrington P.H., 1996, *Comput. Phys. Commun* 92, 290
- Burke V.M., Noble C.J., 1995, *Comput. Phys. Commun.* 85, 471
- Butler K., Zeippen C.J., 1994, *A&AS* 108, 1 (Paper V)
- Clementi E., Roetti C., 1974, *Atom. Data Nucl. Data Tables* 14, 177
- Galavis M.E., Mendoza C., Zeippen C.J., 1995, *A&AS* 111, 347 (Paper X)
- Hibbert A., 1975, *Comput. Phys. Commun.* 9, 141
- Hibbert A., Le Dourneuf M., Vo Ky Lan, 1977, *J. Phys. B: At. Mol. Phys.* 10, 1015
- Hummer D.G., Berrington K.A., Eissner W., Pradhan A.K., Saraph H.E., Tully J.A., 1993, *A&A* 279, 298 (Paper I)
- Lennon D.J., Burke V.M., 1994, *A&AS* 103, 273 (Paper II)
- Li H., McCray R., Sunyaev R.A., 1993, *ApJ* 419, 824
- Nahar S.N., 1995, *A&A* 293, 967 (Paper VII)
- Pelan J., Berrington K.A., 1995, *A&AS* 110, 209 (Paper IX)
- Reader J., Sugar J., 1975, *J. Phys. Chem. Ref. Data* 4, 353
- Saraph H.E., Tully J.A., 1994, *A&AS* 107, 29 (Paper IV)
- Saraph H.E., Storey P.J., 1996, *A&AS* 115, 151 (Paper XI)
- Sawey P.M.J., Berrington K.A., 1992, *J. Phys. B: At. Mol. Phys.* 25, 1451
- Scott N.S., Taylor K.T., 1982, *Comput. Phys. Commun.* 25, 347
- Storey P.J., Mason H.E., Saraph H.E., 1996, *A&A* 309, 677 (Paper XIV)
- Wigner E.P., 1948, *Phys. Rev.* 73, 1002
- Zhang H.L., Graziani M., Pradhan A.K., 1994, *A&A* 283, 319 (Paper III)
- Zhang H.L., Pradhan A.K., 1995, *A&A* 293, 953 (Paper VI)